Active and Reactive Power control in a grid-connected Microgrid with Energy Storage Management

Filipe Perez[1], Lúcio de Medeiros[1], André Pedretti[2]
[1]Lactec, Research & Development, Curitiba, Brazil, filipe.perez@lactec.org.br, lucio.medeiros@lactec.org.br
[2]Copel, Companhia Paranaense de Energia, Curitiba, Brazil, andre.pedretti@copel.com

***Abstract*—The integration of renewable energy sources coordinated with the use of energy storage systems to provide power for a local grid is the main target for microgrids. Microgrids allow better integration of renewable sources, as well as allow adequate management of the storage elements, which bring improvements in power quality of the electrical systems. This paper presents the simulation results of the operation and control of a microgrid consisting of a photovoltaic generation system with energy storage (batteries) and the load in a distribution system. This work is part of the R&D project (Copel, 2016), whose objective is the development of a control system for the management of energy resources and loads of the consumer in the context of intelligent microgrids, as support to the integration of distributed generation. The management method is based on the construction of an optimal control algorithm and a hierarchical control structure of microgrids.**

***Index Terms*—Microgrids, hierarquical control, management system, energy storage, renewable energy.**

I. Introduction

The impacts caused in the electricity network by the integration of distributed generation through renewable sources, together with the development of energy storage technologies and the modernization of electric loads has brought considerable changes in power system operation. Microgrids enable better integration of renewable sources, supply of local loads independently of the network, i.e., island mode operation, through the management of energy storage. Thus, the benefits generated in the use of microgrids bring greater reliability and resilience of the distribution system with better energy efficiency [1], [2], [3].

The great challenge lies in the development of control strategies for operation and management of a microgrid, since the design of the control can become quite complex, being a relevant research topic in this area. A microgrid needs the management of its variables to attain safe operation, in order to guarantee transient stability, as well as the regulation of the power flow, attendance to local load within the network requirements. i.e. frequency and voltage regulation, optimization of distributed generations, reliable operation and robustness to network disturbances [4], [5], [6].

In the development of microgrids projects are defined the size of the load, and from this, the distributed generation and energy storage elements are designed for correct operation

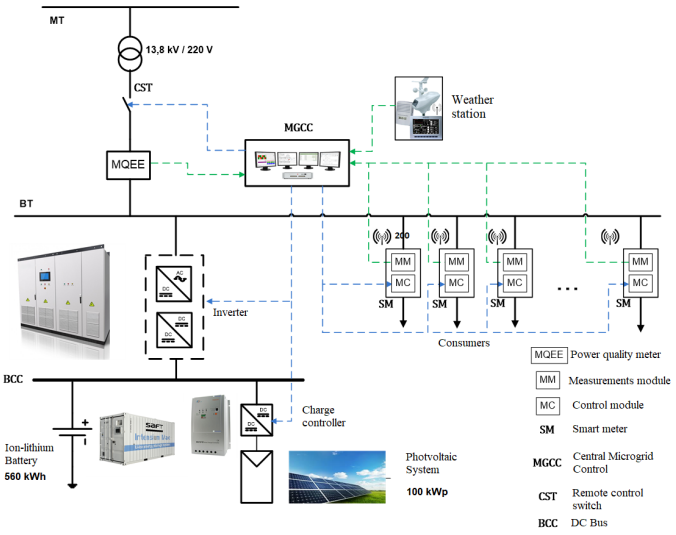

Fig. 1. Proposed system architecture for the R&D project.

of the microgrid. Thus, with the use of energy storage it is possible to control variations of the demand not met by the distributed generation and even the use of load-shedding for critical moments, where it is not possible to feed the system completely, prioritizing important loads [7], [8].

The interest in the application of energy storage systems has grown considerably in Brazil since the public call of the Aneel Strategic call in 2016 (Call 22), which had the objective of proposing technical and commercial arrangements for the evaluation and insertion of Energy Storage Systems (ESS) in the Brazilian electric sector, in an integrated and sustainable way. Considering the increasing insertion of renewable sources, it is envisaged the use of large scale ESS, once proven its technical and economic viability, resulting in impacts reductions and obtaining save and dispachble way for energy supply. In this context, the discussions presented here are part of the first results of one of the R&D projects of Public Call n. 21 (Copel, 2016), focused on the development of a control system for the management of energy storage systems and consumer loads in the context of intelligent microgrids as support for the integration of distributed generation.

A pilot system will be installed in the distributor's concession area, allowing optimal operation considering renewable

978-1-5386-8218-0/19/$31.00

sources, battery banks, priority and controllable loads, as well as other elements of automation, control and power electronics. Fig. 1 presents the proposed architecture for the R&D project.

In this project, the photovoltaic system and critical loads will be considered as non-controllable elements. Then, the storage system will be controlled according to the optimization algorithm, acting through remote control switches and electronic converters. It is planned to use a 100 kWp photovoltaic system and a storage system with lithium-ion batteries of 560 kWh, plus 100 smart meters in consumers loads. A telecommunication infrastructure will be implemented as part of the automation and control system, allowing the remote transmission of real-time monitoring data of electrical and meteorological quantities to the central controller.

This paper discusses the management system of a microgrid, consisting of a set of photovoltaic panels, lithium-ion batteries, a local load and the connection to the main network. The operation of the system aims to adequately feed the system loads, bringing improvement in the parameters of power quality, mainly related and voltage profile, reactive regulation and power factor correction, at the same time optimizing the battery life and performing the maximum energy efficiency of photovoltaic generation. The results of simulations present different modes of operation in the network and verify the microgrid control performance.

II. Hierarchical Structure of Control

In order to guarantee the proper functioning of a microgrid it is necessary to undertake a complete control strategy involving different time-scales, referring to a hierarchical control structure. This structure covers local, primary, secondary, and tertiary controllers, ranging from milliseconds to hours or a day [9], [10], [11].

Local control consists of mathematical algorithms that ensure the stability of lower level variables (voltages and currents) and stabilize perturbations with fast response, good transient performance and steady state regulation. Local controllers ensure the system's transient stability in milliseconds to seconds, following the references of currents and voltages provided by higher level controllers. Local control acts on microgrid converters through PWM modulation to control the dynamics of the converters [12], [13], [14].

The primary control operates in a time interval of a few seconds. Its responsibility is to adapt the operating points of the system to an active disturbance during the time interval in which the secondary controller needs to calculate an ideal new operating setpoint. For smaller microgrids, the primary can be integrated with the local controller through a master-slave approach. In this case, it is assumed that the converter acts as master, maintaining the stability of the network.

The secondary level controller regulates the power flow of the system taking into account the state of charge (SoC) of the energy storage systems (battery). In this way, an optimal power flow is generated. This power flow is calculated by sharing the load demand in the system between the generation of renewable sources and the storage elements, allowing its

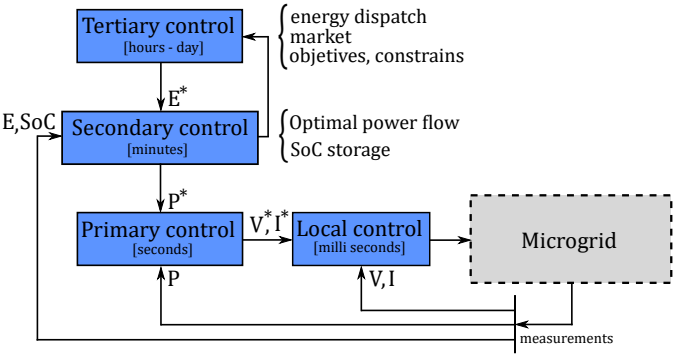

Fig. 2. Hierarchical structure of microgrid control [17].

proper functioning and guaranteeing the increase of the battery life. The secondary control provides a power reference to the network, ensuring the energy balance in the system. The secondary is also related to the power quality requirements and the operational limits of the device in which the restrictions must be respected [11].

The tertiary control works with the energy market, organizing the energy dispatch schedule according to an economic point of view, considering the negotiation between consumers and producers. This level also deals with human-machine interaction and social aspects [15], [16]. Fig. 2 presents a general scheme of hierarchical control for microgrids.

III. Model of the System

The proposed microgrid is composed of a photovoltaic system and lithium-ion batteries connected into Voltage Source Converter (VSC) integrated in the distribution network. The distribution system may be isolated for feeding a local load in the island mode operation. Through the microgrid scheme shown in Fig. 3, the dynamic equations of the system are obtained, as shown below:

The PV is connected to the DC bus via a boost converter. The dynamic equations of the photovoltaic array are introduced into (1)-(2), where V_{PV} is the voltage output of the panel, I_{L_1} is the inductor current, V_{C_1} is capacitor voltage C_1 and d_1 is the duty cycle of the converter.

The battery bank equations are introduced in (3)-(4), where V_{bat} is the battery voltage, I_{L_2} is the inductor current, V_{C_2} is capacitor voltage and d_2 is the duty cycle of the converter. The storage system is integrated into the DC coupling through a bidirectional boost converter.

For the integration of the PV array and the battery bank in the electrical network, a VSC converter is applied. The dynamic equations of the converter are introduced in (5)-(7), where I_d is the direct axis current referring to the active power injected into the network and I_q the quadrature current referring to reactive power injected into the network, within the synchronous reference system (dq). The voltage at the DC coupling is represented by V_{DC}, m_d and m_q are the modulation indices of the converter, ω is the fundamental

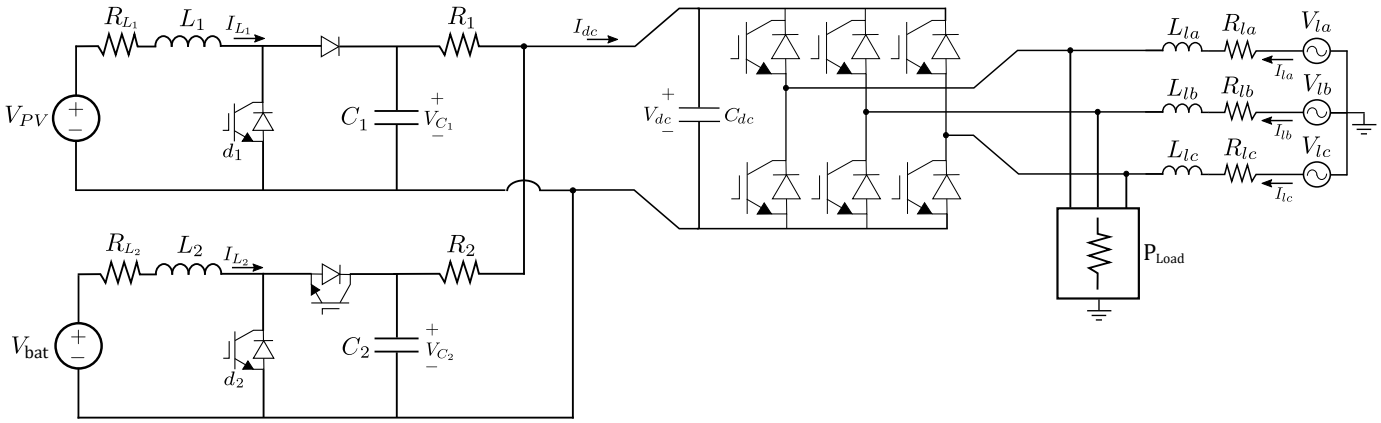

Fig. 3. Proposed microgrid electric scheme.

frequency of the network and V_d and V_q are the synchronous AC voltages.

$$\frac{dI_{L_1}}{dt} = \frac{V_{PV}}{L_1} - \frac{R_{L_1}}{L_1} I_{L_1} - \frac{V_{C_1}}{L_1}(1 - d_1) \tag{1}$$

$$\frac{dV_{C_1}}{dt} = \frac{V_{DC}}{R_1 C_1} - \frac{V_{C_1}}{R_1 C_1} + \frac{I_{L_1}}{C_1}(1 - d_1) \tag{2}$$

$$\frac{dI_{L_2}}{dt} = \frac{V_{bat}}{L_2} - \frac{R_{L_2}}{L_2} I_{L_2} - \frac{V_{C_2}}{L_2}(1 - d_2) \tag{3}$$

$$\frac{dV_{C_2}}{dt} = \frac{V_{DC}}{R_2 C_2} - \frac{V_{C_2}}{R_2 C_2} + \frac{I_{L_2}}{C_2}(1 - d_2) \tag{4}$$

$$\frac{dI_d}{dt} - \frac{R_l}{L_l} I_d + \omega I_q + \frac{V_{C_17}}{2L_l} m_d - \frac{V_d}{L_l} \tag{5}$$

$$\frac{dI_q}{dt} = -\frac{R_l}{L_l} I_q - \omega I_d + \frac{V_{C_17}}{2L_l} m_q - \frac{V_q}{L_l} \tag{6}$$

$$\frac{dV_{DC}}{dt} = \frac{2}{C_{DC}} \left[\frac{1}{R_1}(V_{C_1} - V_{DC}) + \right. \\ \left. + \frac{1}{R_2}(V_{C_2} - V_{DC}) - \frac{3(V_d I_d + V_q I_q)}{2V_{DC}} \right] \tag{7}$$

Thus, I_{L_1}, V_{C_1}, I_{L_2}, V_{C_2}, I_d, I_q, and V_{DC} are the system state variables, d_1, d_2, m_d and m_q are the control inputs and V_{PV}, V_{bat}, V_d, and V_q are the disturbances to this philosophy of control. According to the microgrid management system, the secondary control must provide a maximum power reference $I^*_{L_1}$ for the PV to work at the maximum power point calculated by the MPPT algorithm; a reference current $I^*_{L_2}$ to control the storage system in order to inject/absorb the right amount of power into the electrical network, working in different modes of operation as peak shaving, voltage regulation, reactive power supply, etc. To feed the loads on the AC side properly, the secondary control generates the references I^*_d and I^*_q, in order to control active and reactive power of the network. Finally, the voltage at the DC coupling should be controlled in V_{DC} to maintain the power balance of the microgrid.

In the next section a control law will be introduced to stabilize the dynamics described in (1)-(7), according to the references given by the secondary level of control.

IV. Control strategy

Considering x as the states, x^e as equilibrium point, y as controlled variable, then the error can be defined as $\tilde{x} = x - x^e$:

$$x = [V_{C_1}, V_{C_2}, V_{DC}]^T \tag{8}$$

$$x^e = [I^*_{L_1}, V^e_{C_1}, I^*_{L_2}, V^e_{C_2}, I^*_d, I^*_q, V^*_{DC}]^T \tag{9}$$

$$y = [I_{L_1}, I_{L_2}, I_d, I_q]^T \tag{10}$$

$$d = [V_{PV}, V_{bat}, V_d, V_d]^T \tag{11}$$

where d are the network disturbances.

The PV and battery control systems are similar, with one input and one control output, as shown below:

$$\begin{cases} \dot{x} = f(x, d) + g(x)u \\ y = I_{L_{1,2}} \end{cases} \tag{12}$$

From this, it is possible to develop a control law that stabilizes the dynamics of the proposed microgrid subsystems. Then, in (13) the control input d_1 is calculated in order to linearize the current dynamics I_{L_1} in (1):

$$d_1 = \frac{1}{V_{C_1}}(L_1 v_1 - V_{PV} + R_{L_1} I_{L_1} + V_{C_1}) \tag{13}$$

where v_1 represents a PI controller, and can be formally written as:

$$v_1 = -K_{p_1}(I_{L_1} - I^*_{L_1}) - \alpha_1 \tag{14}$$

$$\dot{\alpha}_1 = -K_{i_1}(I_{L_1} - I^*_{L_1}) \tag{15}$$

The proportional and integral K_{p_1} and K_{i_1}, respectively, gains are calculated to meet the desired performance of control, ensuring convergence and zero steady-state error [13], [18].

The calculation of d_2 for the storage subsystem is done similarly to d_1, written as:

$$d_2 = \frac{1}{V_{C_2}}(L_2 v_2 - V_{bat} + R_{L_2} I_{L_2} + V_{C_2}) \tag{16}$$

and the PI controller is also added to the system as follows:

$$v_2 = -K_{p_2}(I_{L_1} - I^*_{L_2}) - \alpha_2 \tag{17}$$
$$\dot{\alpha}_2 = -K_{i_2}(I_{L_2} - I^*_{L_2}) \tag{18}$$

K_{p_2} and K_{i_2} are proportional and integral gains, respectively, with parameterization in order to achieve the same control performance of the PV system.

The VSC converter connects the PV array and storage system into the distribution system. In this converter, the control of the active power P, and reactive power Q, is done through the currents I_d and I_q, respectively. Thus, according to the control philosophy, the modulation indices m_d and m_q are calculated such that the VSC dynamics are linearized. Then, we can write the VSC modulation indices as:

$$m_d = \frac{2}{V_{DC}}(L_l v_d + R_l I_d - \omega L_l I_q + V_d) \tag{19}$$
$$m_q = \frac{2}{V_{DC}}(L_l v_q + R_l I_q + \omega L_l I_d + V_q) \tag{20}$$

where $v_{d,q}$ represents the insertion of the PI controller, and in a similar way to the previous one, $v_{d,q}$ can be written as:

$$v_{d,q} = -K_{p_{d,q}}(I_{d,q} - I^*_{d,q}) - \alpha_{d,q} \tag{21}$$
$$\dot{\alpha}_{d,q} = -K_{i_{d,q}}(I_{d,q} - I^*_{d,q}) \tag{22}$$

where $k_{p_{d,q}}$ and $K_{i_{d,q}}$ are the proportional and integral gains respectively [19].

In the proposed management model, the storage system receives directly from the secondary control a current reference $I^*_{L_2}$ according to the control objective. Thus, it is necessary for the VSC converter to inject all available power into the DC coupling. The value of the reference current I^*_d should be calculated to provide the desired amount of active power to the network, i.e., I^*_d is calculated such that the DC coupling voltage converts to its reference V^*_{DC}. Inserting a external control loop (cascaded) to the voltage V_{dc} and allocating the voltage dynamics to be much slower than the current dynamics ($I_{d,q}$), it is possible to result in *singular perturbation* analysis. Thus, it is guaranteed that in the dynamic analysis of DC bus voltage, the variable I_d has already reached equilibrium point I^*_d, subsequent to the separation of the time scale. In this case, the gains of the controllers must be allocated in order to guarantee this difference in the time scale between current and voltage.

Then, the dynamic equation of the voltage in the DC coupling can be written as:

$$\dot{V}_{DC} = \Bigg[\frac{1}{R_1}(V_{C_1} - V_{DC}) + \\ + \frac{1}{R_2}(V_{C_2} - V_{DC}) - \frac{3(V_d I^*_d + V_q I^*_q)}{2V_{DC}}\Bigg] \tag{23}$$

In (23), the current I_d is seen as a nine control input, which can be calculated in order to linearize the dynamics of V_{DC} via feedback. Then I^*_d can be written as:

$$I^*_d = \frac{2V_{DC}}{3V_d}\Bigg[-\frac{C_{dc}}{2}v_{dc} + \frac{1}{R_1}(V_{C_1} - V_{DC}) \\ + \frac{1}{R_2}(V_{C_2} - V_{DC}) + \frac{V_q I^*_q}{2V_{DC}}\Bigg] \tag{24}$$

The PI controller is inserted via v_{dc}:

$$v_{dc} = -K_{p_{dc}}(V_{DC} - V^*_{DC}) - \alpha_{dc} \tag{25}$$
$$\dot{\alpha}_{dc} = -K_{i_{dc}}(V_{DC} - V^*_{DC}) \tag{26}$$

In (24), the reference current is found in order to balance the power flow in the DC link and further control V_{DC} in V^*_{DC} through the external control loop of the PI controller [8], [20], [21].

The current I_q is controlled in the reference I^*_q to provide the right amount of reactive power into network since the active and reactive power can be controlled independently. The reference I^*_q is calculated as follows:

$$I^*_q = \frac{2Q^*}{3} \tag{27}$$

where Q^* is the desired reactive power for the network.

After design the control laws, a stability study is provided below for the remaining dynamics of the system. The uncontrolled variables are V_{C_1} and V_{C_2}. Then, we can write the equilibrium points of these dynamics as:

$$V^e_{C_1} = \frac{V_{DC}}{2} \pm \frac{1}{2}\sqrt{V^2_{DC} + 4R_1 I_{L_1}(-V_{PV} + R_{L_1} I_{L_1})} \tag{28}$$

$$V^e_{C_2} = \frac{V_{DC}}{2} \pm \frac{1}{2}\sqrt{V^2_{DC} + 4R_2 I_{L_2}(-V_{bat} + R_{L_2} I_{L_2})} \tag{29}$$

Linearizing V_{C_1} and V_{C_2} around the equilibrium point calculated in (28) and (29) respectively, we can conclude about the local stability of the variables by studying the Jacobian sign of the variables:

$$J_1 = -\frac{1}{R_1 C_1} - \frac{1}{C_1}\frac{I^*_{L_1}}{{V^e_{C_1}}^2}(V_{V_{PV}} - R_{L_1} I_{L_1}) \tag{30}$$

$$J_2 = -\frac{1}{R_2 C_2} - \frac{1}{C_2}\frac{I^*_{L_2}}{{V^e_{C_2}}^2}(V_{bat} - R_{L_2} I_{L_2}) \tag{31}$$

In the equation (30), it can be assumed that the current is always positive I_{L_1}. Then, Jacobian J_1 can be considered to be always negative because the PV voltage is always greater than the voltage losses in the inductor: $V_{PV} > R_{L_1} I_{L_1}$, which is also a physical constraint of the system, so V_{C_1} is locally stable, guaranteeing local stability of this variable [4], [7].

In (31), the current I_{L_2} can assume positive and negative values varying according to the charge/discharge of the battery. Thus, we find the following stability region for V_{C_2}, where the Jacobian J_2 is always negative.

$$\frac{V_{bat}}{2R_{L_2}} - \frac{1}{R_{L_2}}\sqrt{\Delta_1} < I_{L_2} < \frac{V_{bat}}{2R_{L_2}} + \frac{1}{R_{L_2}}\sqrt{\Delta_1} \tag{32}$$

where $\Delta_1 = V^2_{bat} + 4\frac{R_{L_2}}{R_2}$.

In conclusion, the uncontrolled dynamics have a stable equilibrium point within the constraints mentioned.

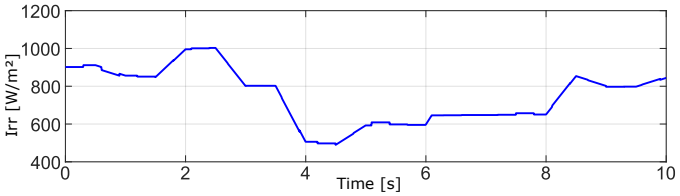

Fig. 4. Irradiation incident on the solar panel.

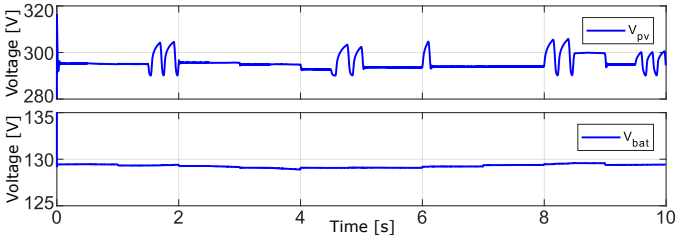

Fig. 5. Voltage in the photovoltaic panel V_{PV} and battery voltage V_{bat}.

V. Simulation Results

It was developed in Matlab/Simulink environment the proposed microgrid from the electrical scheme presented in Fig. 3. The simulated photovoltaic system has 330 panels of 305 Wp, totaling 100 kWp of generation. The storage system is composed of a 10 cells lithium-ion bank of 220 Ah capacity and 12 V nominal voltage, resulting 120 V on the battery bank. The modeled distribution network is represented as a three-phase AC bus with 220 V rms voltage, nominal frequency of 60 Hz and short circuit power of 1 MVA. The selected local load consists of 6 consumer units with nominal active power of 135 kW and 2 $kVAr$ of reactive power.

The Fig. 4 shows the irradiation profile on the PV array, representing the solar oscillations during the day. The nominal irradiation is 1000 W/m^2.

The Fig. 5 shows the voltage in the photovoltaic panel and the battery voltage, respectively. The voltage variations in the PV are caused by the MPPT adjusting the new points of maximum power and the voltage in the battery is maintained with small variations.

Fig. 6 shows the current I_{L_1} in the solar panel (in blue) and the current I_{L_2} of the battery (in red). The PV current I_{L_1} has the same profile from the irradiation presented in Fig. 4. It is notice that large variations can cause great impacts of fluctuation in the power injected into the system. The battery current I_{L_2} absorbs these variations in order to deliver the power required for local charging. The battery acts as a reservoir that brings the power flow balance to the network.

The energy balance on the microgrid is assured by the voltage regulation in the DC bus, and the power mismatch can cause deviation on the DC bus voltage compromising the power flow balance. The voltage on the DC bus V_{DC} is controlled at a constant value ($V_{DC} = 500\ V$). Fig. 7 shows DC bus voltage and its reference, where variations occur due to grid disturbances, variations in PV generation or by load shift demand. The voltage V_{DC} is well controlled

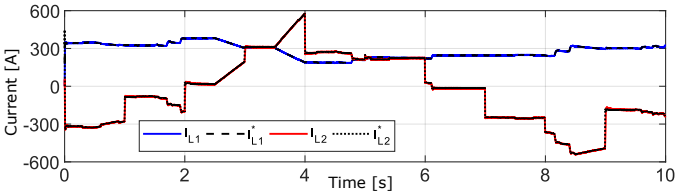

Fig. 6. PV currentI_{L_1} and battery current I_{L_2} with their references.

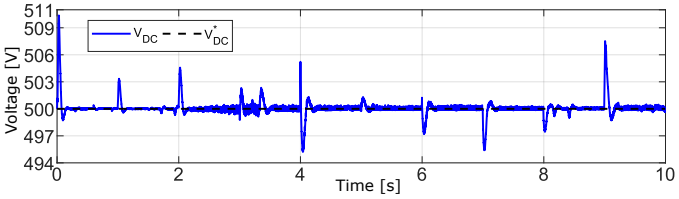

Fig. 7. Controlled voltage on the DC bus V_{DC} and its reference V^*_{DC}.

with 4% of maximum error, ensuring good operation of the microgrid devices (PV and battery) and supplying power to the distribution system correctly.

The direct axis current is proportionally related to the active power in the AC network. In this case, I_d is the current at the coupling point (PCC) that interconnects the microgrid, the network and the load. Current I_q can be used to provide ancillary services (e.g., voltage regulation and power factor regulation). Fig. 8 shows the currents I_d and I_q respectively. The reference I^*_d is calculated by the external control loop in order to guarantee stability in the DC bus, relating the power supplied and the power demanded by the load. The current I_q varies according to the reactive power demand, both variables have good control performance.

The Fig. 9 shows the rms voltage at the PCC and the current injected into the network in p.u., respectively. The voltage present small variations being almost constant in its nominal value, and the current varies in order to guarantee the AC load supply. The voltage base is $V_{base} = 220\ V$ and the power base is $S_{base} = 200\ kVA$.

Finally, Fig. 10 shows the active power $P_{microgrid}$ injected into the network given by the PV and battery generation; the power demanded by the local load P_{load}; and the power supplied by the main grid P_{grid} to meet the power demand. It is noted that the power generated by the microgrid follows the same profile of the power demanded by the load, therefore the use of the main grid relieved by the microgrid. Thus, in this operation mode, the microgrid is adequately providing services

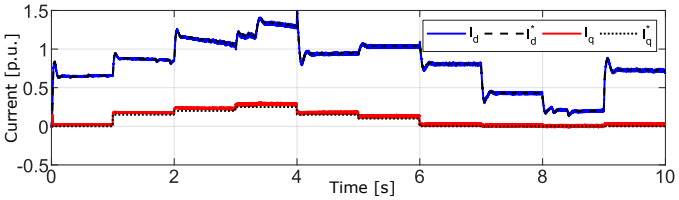

Fig. 8. Direct current I_d, quadratic current I_q with their references.

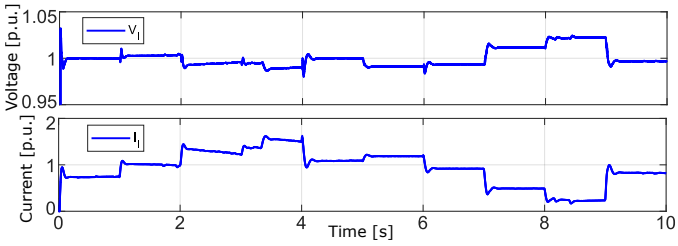

Fig. 9. Rms voltage on PCC and injected current into the AC grid.

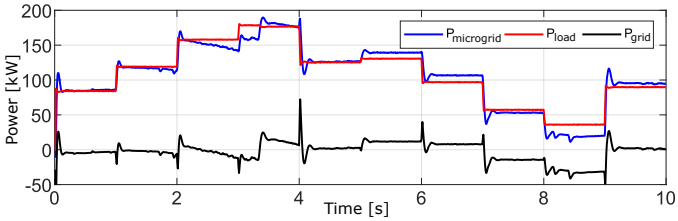

Fig. 10. Power balance in the grid: generation, load and network.

to the main grid improving the system operation and power quality.

VI. Conclusions

This paper discusses the development of a microgrids management system based on a hierarchical control structure, addressing system stability at local and primary level, considered as an optimized secondary control. The proposed microgrid consists of a photovoltaic system and a bank of batteries connected to a local load of the distribution system by means of a VSC converter, allowing operation in mode connected with the electric network.

The proposed control structure allows the PV to extract the maximum power for injection in the network, supply the load in order to meet the network requirements and control the battery to balance the power flow of the system and optimize the operation of the microgrid. The control strategy developed is done by linearization via feedback, guaranteeing transient stability within the region of operation of the microgrid. Simulation results show the microgrid control performance and the correct operation of the microgrid.

Acknowledgment

This work was financed by the Companhia Paranaense de Energia - COPEL research and technological development program, through R&D project 02866-0442 / 2017, regulated by ANEEL.

References

[1] L. E. Zubieta, "Are Microgrids the Future of Energy?: DC Microgrids from Concept to Demonstration to Deployment," *IEEE Electrification Magazine*, vol. 4, no. 2, pp. 37–44, June 2016.

[2] R. H. Lasseter, "Smart distribution: Coupled microgrids," *Proceedings of the IEEE*, vol. 99, no. 6, pp. 1074–1082, 2011.

[3] F. Perez, G. Damm, F. Lamnabhi-Lagarrigue, and P. Ribeiro, "Nonlinear control for isolated dc microgrids," *Revue Africaine de la Recherche en Informatique et Mathématiques Appliquées, INRIA, inPress, Special Issue "MADEV Health and Energy"*, vol. 30, Aug 2018.

[4] A. Iovine, S. B. Siad, G. Damm, E. De Santis, and M. D. Di Benedetto, "Nonlinear Control of a DC MicroGrid for the Integration of Photovoltaic Panels," *IEEE Transactions on Automation Science and Engineering*, vol. 14, no. 2, pp. 524–535, April 2017.

[5] E. Rokrok, M. Shafie-Khah, and J. P. S. Catalão, "Comparison of two control strategies in an autonomous hybrid microgrid," in *2017 IEEE PES Innovative Smart Grid Technologies Conference Europe (ISGT-Europe)*, Sept 2017, pp. 1–6.

[6] M. Tucci, S. Riverso, and G. Ferrari-Trecate, "Line-independent plug-and-play controllers for voltage stabilization in dc microgrids," *IEEE Transactions on Control Systems Technology*, vol. 26, no. 3, pp. 1115–1123, May 2018.

[7] A. Iovine, S. B. Siad, G. Damm, E. De Santis, and M. D. Di Benedetto, "Nonlinear control of an AC-connected DC MicroGrid," in *IECON 2016 - 42nd Annual Conference of the IEEE Industrial Electronics Society*, Oct 2016, pp. 4193–4198.

[8] K. F. Krommydas and A. T. Alexandridis, "Modular Control Design and Stability Analysis of Isolated PV-Source/Battery-Storage Distributed Generation Systems," *IEEE Journal on Emerging and Selected Topics in Circuits and Systems*, vol. 5, no. 3, pp. 372–382, Sept 2015.

[9] A. Iovine, T. Rigaut, G. Damm, E. De Santis, and M. D. Di Benedetto, "Power Management for a DC MicroGrid integrating Renewables and Storages," *submitted to Control Engineering Practice*, 2017.

[10] R. F. Bastos, T. Dragičević, J. M. Guerrero, and R. Q. Machado, "Decentralized control for renewable DC Microgrid with composite energy storage system and UC voltage restoration connected to the grid," in *IECON 2016 - 42nd Annual Conference of the IEEE Industrial Electronics Society*, Oct 2016, pp. 2016–2021.

[11] L. Meng, M. Savaghebi, F. Andrade, J. C. Vasquez, J. M. Guerrero, and M. Graells, "Microgrid central controller development and hierarchical control implementation in the intelligent microgrid lab of aalborg university," in *2015 IEEE Applied Power Electronics Conference and Exposition (APEC)*, March 2015, pp. 2585–2592.

[12] D. E. Olivares, A. Mehrizi-Sani, A. H. Etemadi, C. A. Cañizares, R. Iravani, M. Kazerani, A. H. Hajimiragha, O. Gomis-Bellmunt, M. Saeedifard, R. Palma-Behnke, G. A. Jiménez-Estévez, and N. D. Hatziargyriou, "Trends in microgrid control," *IEEE Transactions on Smart Grid*, vol. 5, no. 4, pp. 1905–1919, July 2014.

[13] F. Perez, A. Iovine, G. Damm, and P. Ribeiro, "DC microgrid voltage stability by dynamic feedback linearization," in *2018 IEEE International Conference on Industrial Technology (ICIT)*, Feb 2018, pp. 129–134.

[14] J. Wang, C. Jin, and P. Wang, "A uniform control strategy for the interlinking converter in hierarchical controlled hybrid ac/dc microgrids," *IEEE Transactions on Industrial Electronics*, vol. 65, no. 8, pp. 6188–6197, Aug 2018.

[15] H. Wen, K. Zheng, and Y. Du, "Hierarchical coordinated control for dc microgrid with crowbar and load shedding control," in *2017 IEEE 3rd International Future Energy Electronics Conference and ECCE Asia (IFEEC 2017 - ECCE Asia)*, June 2017, pp. 2208–2212.

[16] X. Yang, F. Tang, X. Wu, and X. Jin, "Hierarchical control strategy of grid-connected dc microgrids," in *2016 IEEE 8th International Power Electronics and Motion Control Conference (IPEMC-ECCE Asia)*, May 2016, pp. 3723–3727.

[17] F. Perez and G. Damm, "Dc microgrids," in *Microgrids Design and Implementation*. Springer, 2019, pp. 447–475.

[18] Y. Chen, G. Damm, A. Benchaib, M. Netto, and F. Lamnabhi-Lagarrigue, "Control induced explicit time-scale separation to attain dc voltage stability for a vsc-hvdc terminal," in *IFAC Proceedings Volumes (IFAC-PapersOnline)*, vol. 19, 08 2014.

[19] H. K. Khalil, *Nonlinear control*. Prentice Hall, 2014.

[20] H. J. Sira Ramirez and R. Silva-Ortigoza, *Control design techniques in power electronics devices*. Springer, 2006.

[21] A. Iovine, G. Damm, E. De Santis, M. D. Di Benedetto, L. Galai-Dol, and P. Pepe, "Voltage Stabilization in a DC MicroGrid by an ISS-like Lyapunov Function implementing Droop Control," in *ECC 2018 - European Control Conference*, Jun 2018.